CONNECTIONIST MODELLING FOR ANTHROPOGENIC GREENHOUSE GASES (GHG) EMISSIONS IN URBAN ENVIRONMENTS

AL-HARBI, M.[1*] – BIN SHAMS, M.[2] – ALHAJRI, I.[3]

[1]*Department of Environmental Technology Management, College of Life Sciences, Kuwait University, P.O. Box 5969, Safat 13060, Kuwait*

[2]*Department of Chemical Engineering, University of Bahrain, P.O. Box 32038, Isa Town, Kingdom of Bahrain*

[3]*Department of Chemical Engineering, College of Technological Studies, P.O. Box 42325, Shuwaikh 70654, Kuwait*

[*]*Corresponding author*
e-mail: dr.meshari@ku.edu.kw

(Received 11th May 2019; accepted 4th Dec 2019)

Abstract. Global warming induced by greenhouse gases (GHGs) is already a reality and will continue to increase resulting in a severe climate change. The aim of the paper is twofold. First, to investigate the GHGs emissions between the year of 2004 and 2016 in four major urban cities, representing the residential band of Kuwait. Results showed a clear steady yearly increase in GHGs emissions, with more emissions in summer compared to winter, possibly due to the high consumption rate of fossil fuel for cooling purposes and traffic activities. Results also revealed a diurnal variation in GHGs emissions, plausibly attributed to the combined effects of busy traffic hours as well as respiration by the living organisms and/or from soils. A second objective in this paper is, to develop a reliable connectionist models such as neural networks for predicting GHGs emissions. Radial basis function (RBF) network due to its known approximation capabilities, localization of its transfer functions and its efficient training algorithms, showed a superior performance in predicting GHGs emissions. Parity and time series plots of the predicted concentrations against the observed concentrations demonstrated the appropriateness of connectionist modelling as a fast and precise tool for monitoring and forecasting the GHGs emissions.
Keywords: *GHGs trend, CO_2 and CH_4 emissions, artificial neural network, radial basis function, model performance*

Introduction

The threat of global warming induced by human-driven emissions of carbon dioxide (CO_2), methane (CH_4), and other greenhouse gases, as well as land-use changes, has become a reality acknowledged by billions of people. Although it is established that 57% of man-made CO_2 emissions can be removed by the biosphere and oceans (Walsh et al., 2017), the level of atmospheric CO_2 has increased progressively through the years as a result of human activities, including deforestation, combustion of fossil fuels, and power generation (Balch et al., 2016; Sterman et al., 2018). Methane atmospheric concentrations have increased by almost 150% since pre-industrial times, which corresponds to a radiative force of $0.48 Wm^{-2}$ (Jędrysek et al., 2015). Based on current trends, extreme events such as temperature extremes, heat waves, and heavy rains are likely to increase in both frequency and intensity. This will eventually induce a rise in Earth's temperature, including its seas.

http://www.aloki.hu ● ISSN 1589 1623 (Print) ● ISSN1785 0037 (Online)
DOI: http://dx.doi.org/10.15666/aeer/1802_20872107

Continuous monitoring of global warming-induced emissions has become an urgent step in mitigating and managing such emissions. Several attempts have been made to monitor the changes of atmospheric CO_2 and CH_4 in different regions around the world. As for 2016 (WDCGG, 2018), CO_2 records were reported as follows: Italy (427.6 ppm), Poland (427.7 ppm), Korea (416.3 ppm), Hungary (410 ppm), and Hong Kong (408 ppm). In India (region of Ahmedabad), CO_2 concentrations varied between 382 and 609 ppm with the annual average of 413 ± 13 ppm during the period of November 2013 to May 2015 (Chandra et al., 2016). In Pakistan, a significant increase in CO_2 concentration was noted from January 2010 (390 ppm) to December 2015 (400 ppm), leading to an increase of 1.75 ppm/year (Mahmood et al., 2016). Similar observations were also reported in South Korea (Shim et al., 2018). CH_4 trend was also investigated in different cities over the world and results revealed a steady increase with a range of 1.95 to 2.10 ppm as of the year of 2016 (WDCGG, 2018). Tracking the trend of GHGs at least during the past three decades, it reveals an increase in the level of greenhouse gases (GHGs) worldwide.

Thus, it is imperative to develop novel and better techniques to estimate concentrations of global warming-induced gases like CO_2 and CH_4. Several approaches have been suggested to model and forecast atmospheric gases. These include for example the atmospheric dispersion model (Loh et al., 2008), statistical regression models that determine the underlying relationship between a set of input data (predictors) and targets (predictands) (Mason and Baddour, 2008), and artificial neural network- based models (ANN) to predict future pollutant concentrations (Ozcan et al., 2006; Kunt et al., 2016; Zhang and Ding, 2017). Notably, ANN has shown promising results and gained more attention in recent years due to its superiority in modelling nonlinear correlations between input and output variables (Amoura et al., 2011; Nezhad et al., 2011; Zhang et al., 2016; Parvizi et al., 2018). ANN has numerous advantages over traditional phenomenological or semi–empirical models. One is its rapid information processing and ability to develop the mapping of input and output variables (Guclu and Dursun, 2010). Other features include the ANN's higher accuracy in predictions over other types of models (Noor et al., 2018) and its ability to handle huge and complex systems within many interrelated parameters (Tahboub et al., 2016).

Due the powerful, accurate, and fast prediction algorithm, ANN models have been used to forecast different pollutant concentrations (Wu et al., 2011) on numerous time scales with acceptable results. Hassan and Dong (2018) predicted the tropospheric ozone (O_3) concentrations using ANN as a function of meteorological conditions and several air quality parameters. Sahin et al. (2004) used the multi-layer perception neural network (MLP-NN) model to predict the daily level of carbon monoxide (CO) in Turkey (Istanbul) using meteorological parameters as predicators. Pawul and Sliwka (2016) applied ANN to predict the concentrations of benzene, CO, and nitrogen oxides (NOx). Elminir and Abdel-Galil (2006) modeled particulate matter (PM_{10}), CO, and nitrogen dioxide (NO_2) based on different climatological variables in Egypt. Rahimi (2017) applied MLP-NN to predict NO_2 in Tabriz, Iran. Several other researchers have used NN techniques to forecast pollutant concentrations (Kurt and Oktay, 2010; Elangasinghe et al., 2014; Russo et al., 2015; Zhao et al., 2018) and the consensus is that an NN can be a useful tool for predicting atmospheric pollutants.

The aim of the present study is twofold. Firstly, to provide a descriptive picture of the current and the trend of GHG's emission in four representative urban areas in Kuwait. Secondly and most importantly, to develop practical, robust, and effective neural networks that forecast the concentration of GHG, specifically, CO_2 and CH_4 emissions in

http://www.aloki.hu ● ISSN 1589 1623 (Print) ● ISSN1785 0037 (Online)
DOI: http://dx.doi.org/10.15666/aeer/1802_20872107

Kuwait. In order to accomplish this, the hourly, daily, seasonal, and yearly records of CO_2 and CH_4 emissions along with their meteorological conditions for the 13-year period were statistically investigated in four major urban cities, representing the residential band of Kuwait. Throughout the investigation, several combinations of artificial neural network (ANN) structures and types, including linear (L), multilayer perception (MLP), and radial basis function (RBF) networks, were tested and optimal models were selected. The neural networks were trained until the network training error achieved the specified acceptable error. The developed NN models in this study yielded feasible, reliable, and efficient prediction of CO_2 and CH_4 concentrations.

Methodology

Study areas

Kuwait is situated in western Asia, between latitudes 28°30'and 30°5' North and longitudes 46°33' and 48°30' East, with a total area of 17,818 km^2. It is bounded by Saudi Arabia in the south and southwest and with Iraq in north and northwest. The total population of Kuwait as of 2018 is about 4.56 million; of whom 1.38 million Kuwaitis and 3.18 million are expatriates. Kuwait's economy is heavily reliant on oil exports through its three refineries, namely Mina Al-Ahmadi (MAA), Mina Abdullah (MAB) and Mina Shuaiba (SHU). These three refineries with a total capacity of 936,000 bpd produce of a variety of refining products to fulfil the international client's needs. Fossil fuels combustion of and fugitive emissions release from oil and gas operations are most prevailing sources of GHG emissions in Kuwait. In this study, to gain overall picture about the trend of GHG in Kuwait, four representative urban areas spatially distributed along the residential band in Kuwait, were selected. These urban areas are Ali Sabah Al-Salem (far-south), Al-Riqqa (South-middle), Mansouriya (Middle), and Al-Jarha (far north), see *Figure 1*. Ali Sabah Al-Salem area is the last inhabited city in the south of Kuwait toward the borders with Saudi Arabia. It is next to highest capacity oil refineries (Mina Al-Ahamdi and Mina Abdullah) in the country. It is also adjacent to several small to large petrochemical industries. This city is surrounded from east by express highway (No.30) and by express highway (No.40) in west, which afterward merges together in one road (No.40) leading to Saudi Arabia borders. The residential area of Al-Riqqa is surrounded by numbers of residential areas in south, north, and west. In east, it is overlooking express highway (No.30) that extends from downtown of Kuwait to borders with Saudi Arabia. In south, it is also proximate to oil refineries (Mina Al-Ahamdi and Mina Abdullah). Al-Riqqa is adjacent to various small to middle scale commercial and industrial areas (e.g. car mechanics). Mansouriya residential area is located in the middle of Kuwait City with a total population of 8992. Mansouriya is typical residential area surrounded with a network of roads in north, south, and east. In west, it is facing express highways No. 40 which cross most of residential areas and connect the city center with south border of Kuwait. The city is few kilometers from numerous commercial buildings and famous traditional shopping centers. In North-West of Mansouriya, there are quite numbers of small-medium industrial business. Al-Jarha city is located in north-west of Kuwait City and it is one of the largest cities in Kuwait with total inhabitants of about 484,502 residents. It is surrounded by numerous emission sources such as Al-Jarha wastewater treatment, desalination and power plans, and different scales of industrial and commercial shops. Numbers of express highway pass through the city include 6^{th} ring

http://www.aloki.hu ● ISSN 1589 1623 (Print) ● ISSN1785 0037 (Online)
DOI: http://dx.doi.org/10.15666/aeer/1802_20872107

road, highway 80 that connects the city to Abdali on the Iraqi border and highway No.70 that links the city to Kuwait border with Saudi Arabia.

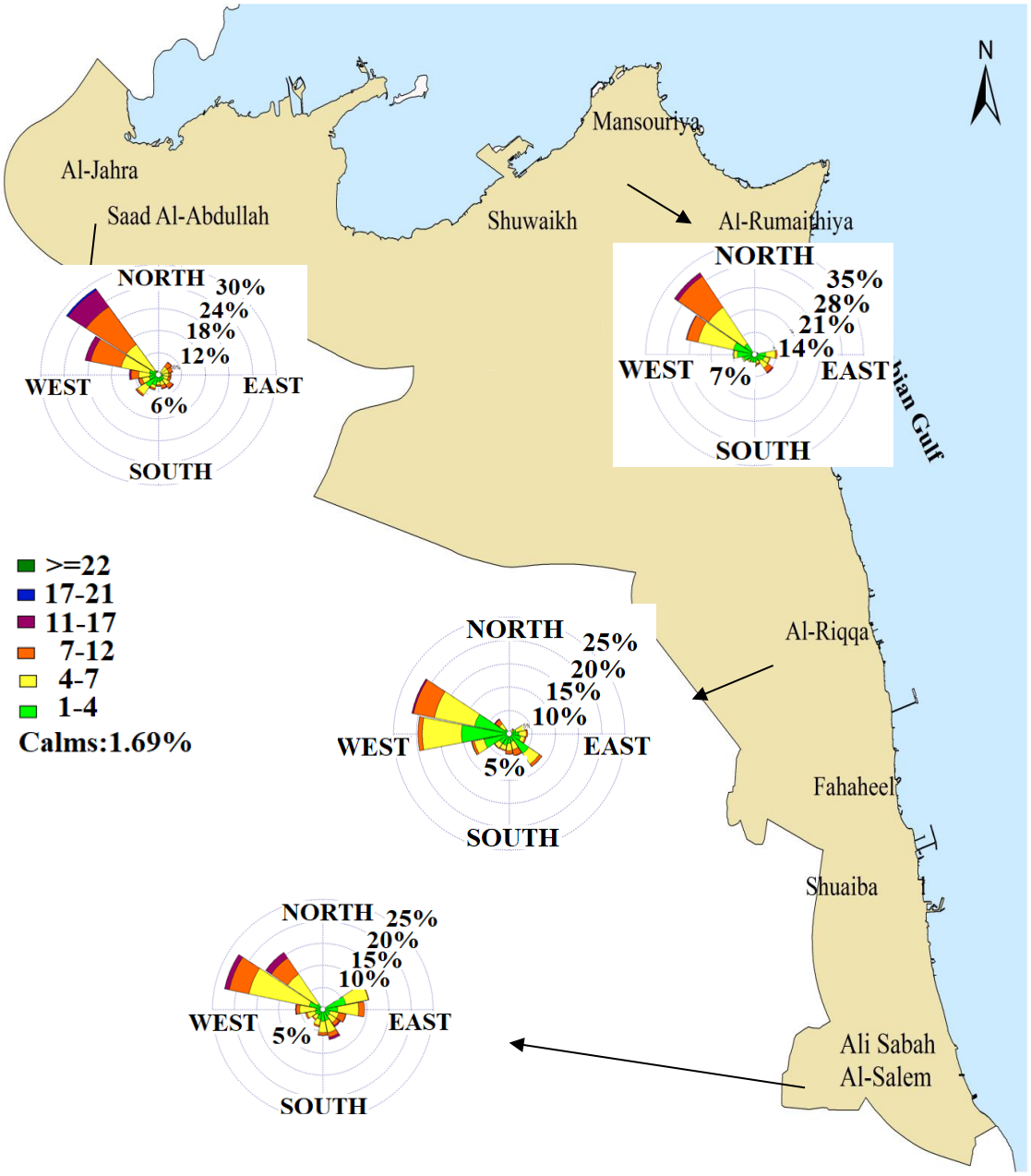

Figure 1. *Selected monitoring sites for quantifying and modeling of Greenhouse gases (GHGs) emissions*

Meteorological conditions

Kuwait is characterized by a desert-type environment and hot climate. Kuwait is experienced sharply by two distinct seasons; summer which last from May to October and winter which extends from November to April. Kuwait is typically arid with very hot summers, with average temperatures vary from 42 to 46°C. In winter, the weather is usually mild to relatively cold with temperatures from time to time even falling below

http://www.aloki.hu ● ISSN 1589 1623 (Print) ● ISSN1785 0037 (Online)
DOI: http://dx.doi.org/10.15666/aeer/1802_20872107

4°C. Dust storms and high concentration of particulate matter (PM) are prevailing characteristic of summer in Kuwait. Humidity is a unique feature of Kuwait climate, starts mid-August and last over September. Over at least the past two decades, relative humidity (RH) ranged from 47.5 and 49.5%, with mean yearly maxima varying from 84 to 95%. From one year to other, RH level could exceed 95%, which is ascribed to high seawater temperatures coincident with tropospheric temperature inversions.

Figure 1 shows wind rose plots for residential areas of Ali Sabah Al-Salem, Al-Riqqa, Mansouriya, and Al-Jarha, for the year of 2016. It is apparent that the prevailing wind directions were strongly northwest winds (~25-33% of time) and mild south to southeasterly winds (~23-28% of time). The average wind speeds (*Table 1*) varied from 2.5± 0.4 m/s to 3.8± 0.5 m/s in summer and between 1.6 ± 0.23 m/s and 2.9 ± 0.22 m/s in winter. In terms of seasonal variation, there is no marked variation in the wind direction throughout the year (*Table 1*).

Table 1. *Descriptive statistics of greenhouse gases (GHG) and climate conditions*

	Summer					Winter				
Ali Sabah Al-Salem	**Min.**	**Mean**	**SD**	**Max.**	**C.V**	**Min.**	**Mean**	**SD**	**Max.**	**C.V**
CO_2 (ppm)	388	428	17	435	0.04	382	412	9.6	420	0.02
CH_4 (ppm)	1.82	2.15	0.12	2.6	0.06	1.80	2.10	0.22	2.35	0.1
Temperature (ºC)	25.5	34.6	4.6	38.5	0.13	12.7	18	5	27.6	0.3
RH	26.6	29.4	2.1	32.7	0.07	26.3	42	14.6	61.4	0.4
Wind speed (m/s)	2.6	2.95	0.4	3.6	0.12	2.26	2.5	0.16	2.72	0.1
Wind direction (Deg.)	45	200.8	92	335	0.44	52	219	87	331	0.40
Al-Riqqa	**Min.**	**Mean**	**SD**	**Max.**	**C.V**	**Min.**	**Mean**	**SD**	**Max.**	**C.V**
CO_2 (ppm)	402	430	12	440	0.03	410	418	24.6	467	0.06
CH_4 (ppm)	1.83	2.25	0.2	2.70	0.1	1.79	2.11	0.21	2.50	0.01
Temperature (ºC)	27.3	37	5	41	0.13	14.8	19.5	5.2	30	0.3
RH	16	23	5.6	33	0.3	28.7	42.6	6.5	48.3	0.2
Wind speed (m/s)	2.03	2.5	0.4	3.14	0.14	1.32	1.65	0.23	1.97	0.1
Wind direction (Deg.)	42	223	76	322	0.34	42	218	70	316	0.32
Mansouriya	**Min.**	**Mean**	**SD**	**Max.**	**C.V**	**Min.**	**Mean**	**SD**	**Max.**	**C.V**
CO_2 (ppm)	394	429	16	429	0.04	385	417	27	431	0.06
CH_4 (ppm)	1.92	2.20	0.1	2.21	0.05	1.98	2.0	0.12	2.36	0.05
Temperature (ºC)	28.7	37.6	4.5	41.6	0.12	16.2	20.8	5.14	31	0.3
RH	29.7	35.1	4.2	42.5	0.12	43.7	56	7.8	67	0.1
Wind speed (m/s)	2.3	2.7	0.34	3.4	0.13	2.1	2.3	0.2	2.5	0.05
Wind direction (Deg.)	69	242	80	324	0.33	67	241	79	324	0.33
Al-Jarha	**Min.**	**Mean**	**SD**	**Max.**	**C.V**	**Min.**	**Mean**	**SD**	**Max.**	**C.V**
CO_2 (ppm)	387	398	3.5	410	0.01	380	390	7.2	399	0.02
CH_4 (ppm)	1.80	1.92	0.08	1.98	0.04	1.77	1.87	0.02	1.93	0.01
Temperature (ºC)	27	35.8	4.5	39.8	0.12	13.7	18.5	5.1	28.7	0.3
RH	7.85	12.61	4.7	21	0.4	20.3	32	7.06	42	0.22
Wind speed (m/s)	3.3	3.8	0.5	4.6	0.13	2.53	2.90	0.22	3.25	0.08
Wind direction (Deg.)	15	238	88	353	0.37	15	232	86	353	0.37

http://www.aloki.hu ● ISSN 1589 1623 (Print) ● ISSN1785 0037 (Online)
DOI: http://dx.doi.org/10.15666/aeer/1802_20872107

Data collection and analysis

The dataset for CO_2 and CH_4 were provided by Air Pollution Monitoring Division of the Kuwait Environment Public Authority (KUEPA). The monitoring stations were placed at Ali Sabah Al-Salem (28.957°N 48.154°E), Al-Riqqa (29.146°N 48.107°E), Mansouriya (29.358°N 47.993 °E), and Al-Jarha (29.3366°N 47.6755°E) and they are equipped with a state-of-art sampling devices and analyzers approved by US-EPA with accuracy of 98-99%. The CO_2 and CH_4 emission were measured using a CO_2/ CH_4/H_2O analyzer (Picarro G1301, US) whereas meteorological conditions such as relative humidity, wind speed, wind direction, and temperature were concurrently monitored using mobile monitoring station (Thermo Scientific, USA). Air probe was approximately between 10-15 m above sea level in all urban cities investigated. Measurements were taken at hourly intervals, which resulted in 8760 per year for each CO_2 and CH_4, with a total of 113,880 data points for each CO_2 and CH_4 for the entire period of 13 years (2004-2016). To study the diurnal cycle, the average concentration at each hour (0-23 hrs) was calculated in each urban area for the entire study period. As for seasonal variations, data were split into two prevailing seasons in Kuwait, summer and winter.

Statistical analysis

Descriptive statistical analyses were performed to demonstrate the overall picture of the CO_2 and CH_4 emissions and their corresponding meteorological conditions. Pearson's correlation (R) analysis and one-way analysis of variance (ANOVA) are used to determine whether there are any statistically significant differences between the means of data set with p value < 0.05. All statistical analyses, neural network modellings and model qualification were made using statistical software package (STATISTICA, StatSoft, USA) and R, version R 3.5.1.

Artificial neural network modeling (connectionist modelling)

Significant number of literature have shown different applications of neural networks for solving different types of problems, most of which can be broadly classified into classification, function approximation or prediction problems. The proficiency of neural networks is attributed to its ability to detect patterns and relationships in the data provided to them during the calibration or training phase. Generally, neural networks are classified according to (a) the network topology e.g. feed forward and recurrent architectures, (b) the network transfer function e.g. sigmoid, radial basis (c) the network learning algorithms e.g. supervised or unsupervised learnings (Karray and De Silva, 2004). The neural network architecture is depicted in *Fig. 2*. Parallel and distributed processing units called neurons or nodes are arranged within three layers, namely, input, hidden and output layers. Each neuron in the input layers is connected to the adjacent layer in the hidden layer through connection weights. Similarly, each neuron in the hidden layer is connected to the adjacent hidden layer or to the output layer through connection weights. In fact, these weights are the model parameters to be estimated using the input/output training sets. The output of each neuron is weighted, summed and passed to nonlinear transformation e.g. sigmoid function. For a chosen network's topology and transfer function, the neural network modelling is reduced to the problem of estimating the connection weights among the neurons such that a certain measure of the mismatch between the observed and predicted values is minimized. More specifically, the cumulative error E_c to be minimized may be given as:

http://www.aloki.hu ● ISSN 1589 1623 (Print) ● ISSN1785 0037 (Online)
DOI: http://dx.doi.org/10.15666/aeer/1802_20872107

$$E_c = \frac{1}{2}\sum_{k=1}^{n}\sum_{i=1}^{q}\left(t_i(k) - o_i(k)\right)^2 \quad \text{(Eq.1)}$$

where n is the total number of training points, q is the total number of neurons at the output layer, t_i is the target value and $o_i(k)$ is the network's output from the k^{th} neutron for the i^{th} training point. Accordingly, the optimization problem of the neural network can be formulated as:

$$\min_{\mathbf{w}} E_c = \min_{\mathbf{w}} \frac{1}{2}\sum_{k=1}^{n}\sum_{i=1}^{q}\left(t_i(k) - o_i(k)\right)^2 \quad \text{(Eq.2)}$$

where the vector w contains the network weights between all the neurons of the network. In the present study, two feed forward architectures, namely multilayer perceptron network (MLP) and the radial basis function network (RBFN) have been considered to predict CO_2 and CH_4 concentrations in 4 urban cities in the state of Kuwait (*Fig. 2*).

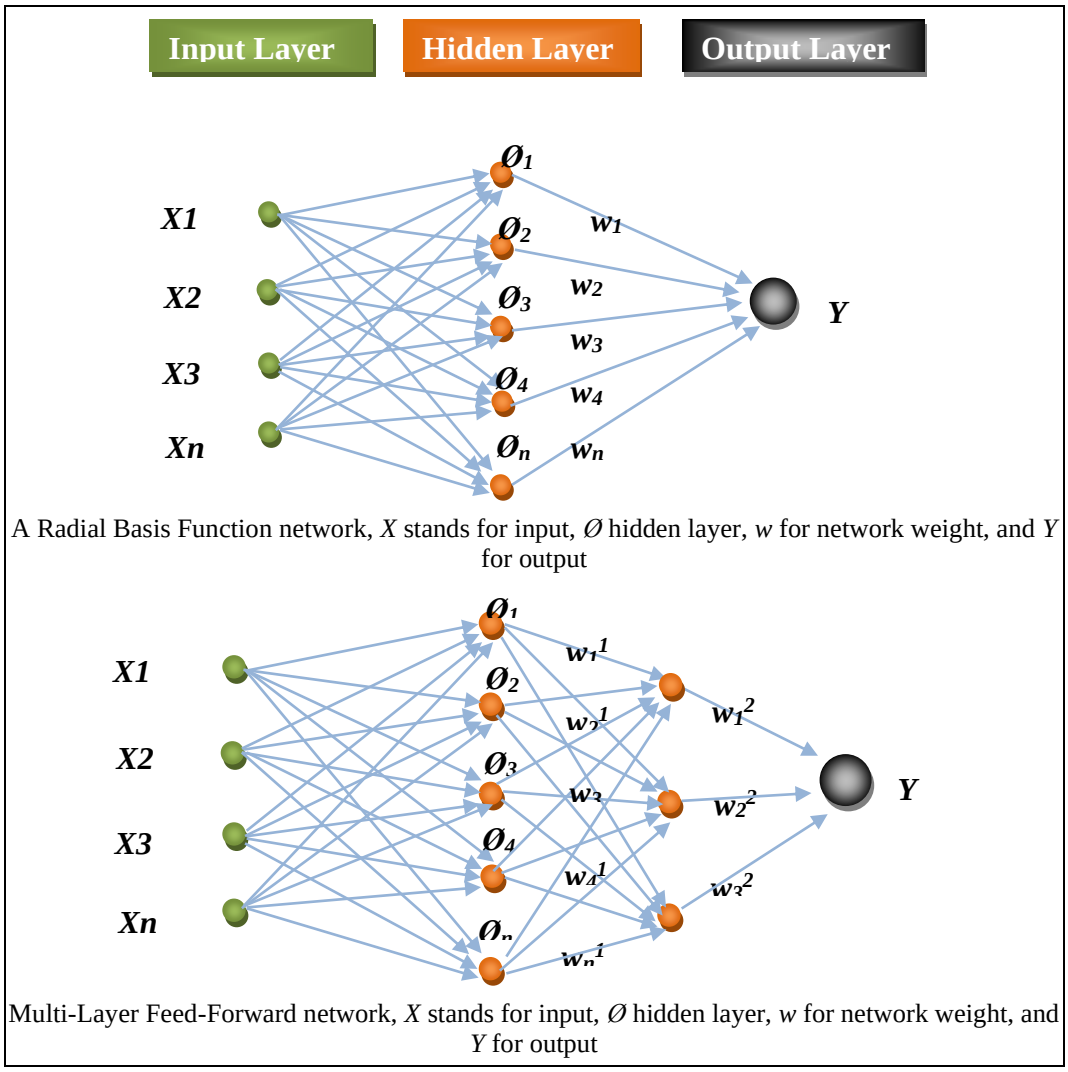

Figure 2. *Architecture of developed artificial neural network (ANN) models*

http://www.aloki.hu ● ISSN 1589 1623 (Print) ● ISSN1785 0037 (Online)
DOI: http://dx.doi.org/10.15666/aeer/1802_20872107

Both, MLP and RBFN are examples of feed forward network with different prediction capabilities (Karray and De Silva, 2004). MLP uses global transfer function such as sigmoid function

$$\text{sigmoid}(x) = \frac{1}{1+\exp(-x)} \quad \text{(Eq.3)}$$

whereas RBFN uses local basis functions such as Gaussian kernel

$$g_i(\mathbf{x}) = \exp\left(\frac{\|\mathbf{x}-\mathbf{v}_i\|^2}{2\sigma_i^2}\right) \quad \text{(Eq.4)}$$

where x is the input vector and v is the center of the radial basis function g_i and σ_i is the width/scaling parameter. While MLP uses back propagation algorithm (supervised learning) to estimate the network weights, RBFN use a two-stage training strategy. In the first stage, the parameters of the radial basis function (v and σ_i) are estimated using unsupervised learning e.g. *k*-means method, while in the second stage the network weights are estimated using gradient methods. A remarkable feature of the RBFN is that the weight between the input and the hidden layers are all equal to one and only the weights between the hidden and the output layer are to be estimated. In the current work, a total of 8,640 hourly concentration readings of CO_2 and CH_4 and their corresponding climatological variables, namely; ambient air temperature, relative humidity, wind speed, and wind direction, were used as input to build the ANN model. About 60% of the total data was used to train the network, 20% was used as a validation set, and the remaining 20% was used as test data. In testing step, the networks have one output, either CO_2 or CH_4 concentration. Training and testing data are normalized before presenting them to the networks. Normalization is an important pre-processing step, in particular, when the input and output variables of the network are of different order of magnitude as can be seen from *Table 1*. Although some rules of thumbs exist for selecting the number of hidden layers and the number of neurons, in practice, the appropriate number is determined through trial and error until certain error criterion is satisfied. There are several advantages of neural networks against other empirical modelling techniques. More importantly is the filtering capacity of neural networks. The reason of the latter is that no single node solely responsible of correlating a certain input to a specific output, but all the nodes contribute differently to the correlation structure extracted from in the input-output pattern presented to the network during the training phase (Baughman and Liu, 1995). On the contrary, for other regression techniques, if one of the variables is missing or very noisy, the model will likely give inaccurate result because each variable is associated with a unique parameter or weight. On the other hand, neural networks suffer from several limitations. The main disadvantage of neural networks is the necessity of large amount of training data. The latter is insignificant if large amount of historical data is available. Another disadvantage of neural networks is that the estimated weights are suboptimal solution, that is, no global solution can be guaranteed. One way to tackle the sub-optimality problem is to reinitiate the weights of the network several times during the training phase until stable weights are obtained.

http://www.aloki.hu ● ISSN 1589 1623 (Print) ● ISSN1785 0037 (Online)
DOI: http://dx.doi.org/10.15666/aeer/1802_20872107

Statistical performance indices

To evaluate the performance of all artificial neural network (ANN) models, commonly used statistical performance indices suggested by the US EPA, such as mean absolute error (MAE), root mean square error (RMSE), and fractional bias (FB) were used (Riswadkar and Kumar, 1994; Patel and Kumar, 1998; Kumar et al., 2006). The MAE is used to measure the closeness of predicted and observed values. In general, the smaller the MAE values, the smaller the difference between the predicted results and the actual data and the better the prediction performance of the network model.

$$\mathrm{MAE} = \frac{1}{\mathrm{n}} \sum_{\mathrm{i}=1}^{\mathrm{n}} \left| \mathrm{P_i} - \mathrm{O_i} \right| \qquad \text{(Eq.5)}$$

With respect to an acceptable model, RMSE values should be small and the RMSE should approach zero in an ideal model. RMSE is commonly used as a measure of the overall model performance:

$$RMSE = \sqrt{\frac{1}{n} \sum_{i=1}^{n} (P_i - O_i)^2} \qquad \text{(Eq.6)}$$

Fractional bias, a non-dimensional factor, is a measure of the difference between the average observed and the average predicted values and is written in symbolic form as:

$$FB = \frac{(\bar{O} - \bar{P})}{0.5(\bar{O} + \bar{P})} \qquad \text{(Eq.7)}$$

The FB parameter varies between -0.5 and +0.5 and a perfect model has an FB value of zero. FB>0 indicates an underestimate in predicted concentrations while FB<0 indicates an overestimate. In equation 5-7, n is the number of data points, P is the predicted data point, and O is the observed data point.

Results and discussion

Trend of GHG emissions in the ambient atmosphere

To gain better insight into the development of GHG emissions in the ambient atmosphere in Kuwait, the yearly mean concentrations for the period of 13 years (2004-2016) were statistically assessed in four representative urban cities (Ali Sabah Al-Salem, Al-Riqqa, Mansouriya, and Al-Jarha), as shown in *Figure 1*. CO_2 yearly mean concentrations in this study were plotted with those measured at the Mauna Loa Observatory in Hawaii for sake of comparison with the world CO_2 trend (*Figure 3a*). Over the period 2004 to 2016, there were considerable increases in the GHG emissions in the urban cities in Kuwait. CO_2 level varies between 342±18 ppm (Ali Sabah Al-Salem) and 350±13 ppm (Al-Jarha) in 2004. The CO_2 concentrations (*Figure 3a*) have shown an upward trend since 2004, with an 11% to 25% increase in 2016 in all urban cities. Prior to 2015, the CO_2 emissions quantified through monitoring networks in urban cities in

http://www.aloki.hu ● ISSN 1589 1623 (Print) ● ISSN1785 0037 (Online)
DOI: http://dx.doi.org/10.15666/aeer/1802_20872107

Kuwait were below those observed at Mauna Loa site (*Figure 3a*). In 2016, the CO_2 emission ranged from 394 ± 10 ppm to 425 ± 14, exceeded CO_2 emissions reported at the Mauna Loa site (404.21 ppm). In terms of CO_2 variation over the years, one-way analysis of variance (ANOVA) showed significant differences (p<0.05) among the urban cities.

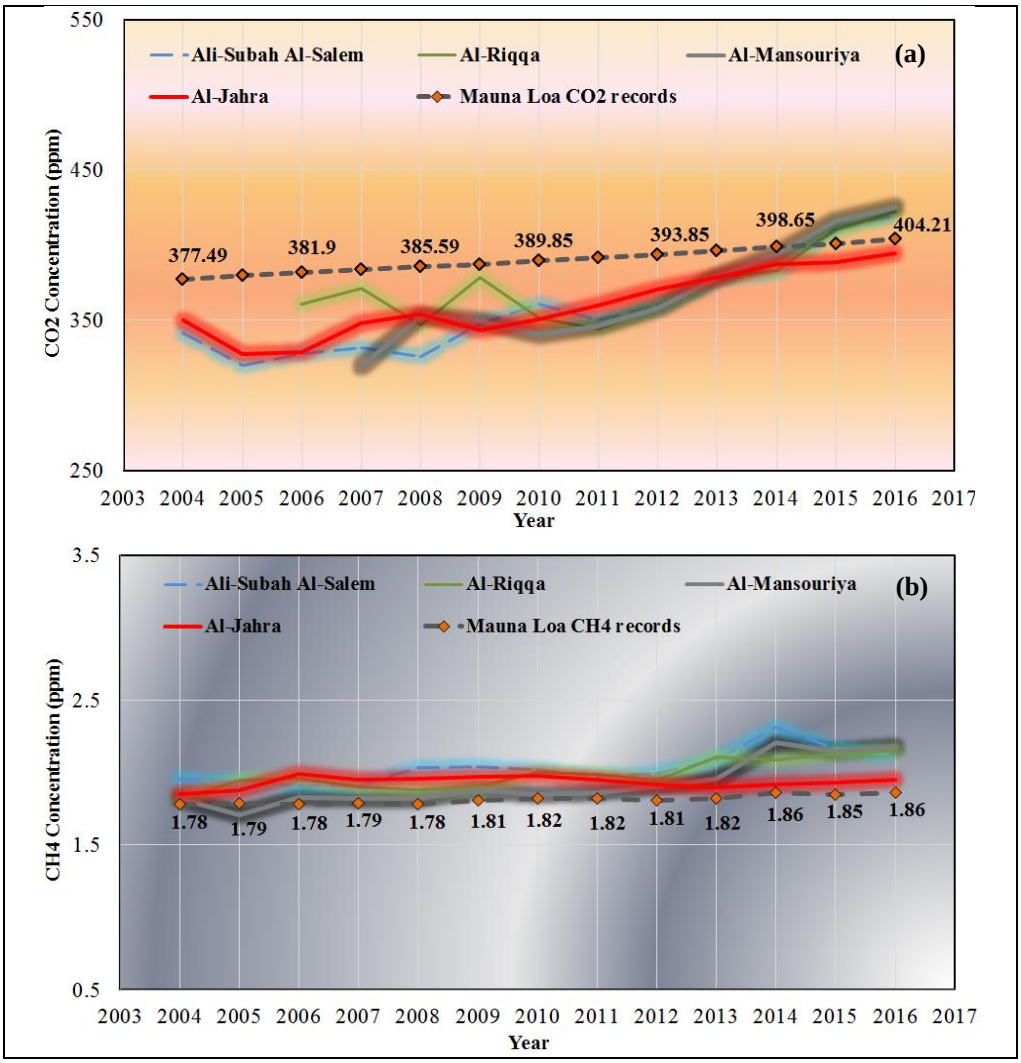

Figure 3. *Yearly trend of (a) CO_2 and (b) CH_4 concentrations in urban areas in Kuwait*

In comparison with other countries in the world, CO_2 levels in this study for the year of 2016 were compared with CO_2 reported in the same year by The World Data Centre for Greenhouse Gases (WDCGG, 2018). The average yearly CO_2 emission in Kuwait was 415.6 ppm, which is lower than those obtained in Poland (427.7 ppm), and Italy (427.6 ppm) and similar to those found in Korea (416.3 ppm), Hungary (410 ppm), Hong Kong (408 ppm), and USA (408 ppm), and higher than those reported in UK (404.6 ppm), Canada (404.5 ppm), Australia (400.8 ppm), and New Zealand (400.6 ppm).

The burning of fossil fuels (oil, gas and coal) for various activities such as transportation, electricity and heat supply, and water treatment is the main source of CO_2 emission in the atmosphere. The magnitude of CO_2 emissions is linked to the carbon content of the fuel as for instance oil and coal has approximately 25% and 40% more

http://www.aloki.hu ● ISSN 1589 1623 (Print) ● ISSN1785 0037 (Online)
DOI: http://dx.doi.org/10.15666/aeer/1802_20872107

carbon content than natural gas, respectively. The extent of CO_2 in the atmosphere is the result of balance of the fluxes between the oceans, the biosphere and the atmosphere. CO_2 circulates from and to the atmosphere via direct absorption/release phenomenon, respiration of plants and the decomposition of organic-matter in soil, and absorption of CO_2 through photosynthesis. To limit the level of atmospheric CO_2 emission, burning of fossil fuels pattern and energy mix should be highly considered.

CH_4 is the second crucial GHG with global warming potential (GWP) of 28 times greater than CO_2 over a 100-year time horizon (IPCC, 2013). It was reported that CH_4 is responsible for about 17% of rise in the total radiative forcing as results of long-lived GHG in the atmosphere during the period of 1750-2016 (WMO, 2017). CH_4 trend, in same urban areas and years span to those of CO_2, was also investigated in Kuwait and results are presented in *Figure 3b*. CH_4 concentrations varied between 1.82±0.09 to 1.94±0.1 ppm in all tested urban areas in Kuwait in 2004. Since 2004, CH_4 concentrations have increased by 100-360 ppb by the end of 2016, with varying rates in the tested urban areas, corresponding to an average range of increase of 8-27 ppb yr^{-1}. It is imperative to note that most CH_4 concentrations observed in all four urban areas exceeded Mauna Loa levels during 2004-2016 (*Figure 3b*). However, the average yearly CH_4 concentration in this study (2.10±0.10 ppm) in the year of 2016 was consistent with CH_4 records reported in other countries in 2016 (WDCGG, 2018) such as Italy (2.00 ppm), Hungary (1.97 ppm), Viet Nam (1.95 ppm), USA (1.97 ppm), and Canada (1.97 ppm). Methane is released to the atmosphere by anthropogenic sources including production and consumption of fossil fuel, biomass burning, and landfills and by natural processes such as wetlands and termites. Conversely, CH_4 level decreases in the atmosphere due to its reaction with hydroxyl radical (OH), persist for about 10 years. Despite the fact that CH_4 is a potent GHG, its influence is comparatively short-lived.

Seasonal and diurnal variation

GHG concentrations were compared in summer and winter, as these are the prevailing season in Kuwait, to learn more about seasonal variability. For the sake of brevity, the comparison in GHG concentrations was limited to 2016. Descriptive statistics of CO_2 and CH_4 concentrations, as well as climate conditions such as temperature, RH, wind speed, and wind direction, during summer and winter for four urban cities are listed in *Table 1*. In summer, the highest mean value of CO_2 emission was 430 ± 12 ppm and found in Al-Riqqa and the lowest value (398 ± 3.5 ppm(was observed in Al-Jahra. In winter, the highest mean value of CO_2 emission was 418 ± 24.6 ppm and observed in Al-Riqqa while the lowest mean value (390 ± 7.2ppm) was found in Al-Jahra. Maximum concentrations of CO_2 (summer = 440 ppm; winter = 467 ppm) were measured in Al-Riqqa while minimum concentrations (summer = 387 ppm; winter = 380 ppm) were found in Al-Jahra. One-way analysis of variance (ANOVA) demonstrated a significant difference ($p<0.05$) between summer and winter in all urban areas in this study. A seasonal variation of CO_2 is obvious in all the urban cities in this study with an overall higher level of CO_2 in summer than winter. This finding is consistent with reported CO_2 in major urban areas (Ghauri et al., 2007; Bergeron and Strachan, 2011). The high CO_2 level in summer is presumably due to the consumption rate of fossil fuel for cooling purposes (e.g., air conditioning) and traffic activities. The temperature in summer reaches 50°C in Kuwait and the air conditioning is in use all day in houses, government buildings, and businesses in the private sector. Increased CO_2 concentration is not restricted to local sources; it can also come from long-range transport from distant source areas.

http://www.aloki.hu ● ISSN 1589 1623 (Print) ● ISSN1785 0037 (Online)
DOI: http://dx.doi.org/10.15666/aeer/1802_20872107

The level of CH_4 in summer and winter was also investigated (*Table 1*). Similar observations to those of CO_2 were reported. The mean concentrations of CH_4 were between 1.92 ± 0.08 ppm and 2.25 ± 0.20 ppm in summer and from 1.87 ± 0.2 ppm and 2.11 ± 0.2 ppm in winter. The highest mean concentration of CH_4 was observed in Al-Riqqa during the summer and winter while the lowest values were found in Al-Jahra. Maximum CH_4 records in summer (2.70 ppm) and in winter (2.50 ppm) were also found in Al-Riqqa. Seasonal differences in all urban cities were statistically significant (ANOVA, $P<0.05$). CH_4 levels in this study exhibited higher levels in summer than in winter in all monitored urban areas (*Table 1*). Such observations were consistent with those reported in different parts of the worlds (Sikar and Scala, 2004; Ito et al., 2005; Ghauri et al., 2007; Satar et al., 2016).

Diurnal variation

Diurnal cycles of GHG emission in the four urban areas for the entire year of 2016 are plotted in *Figure 4a,b* to understand their short-term variability. CO_2 diurnal pattern (*Figure 4a*) in all tested urban localities were almost similar, but vary with magnitudes according to ANOVA analysis ($p<0.05$).

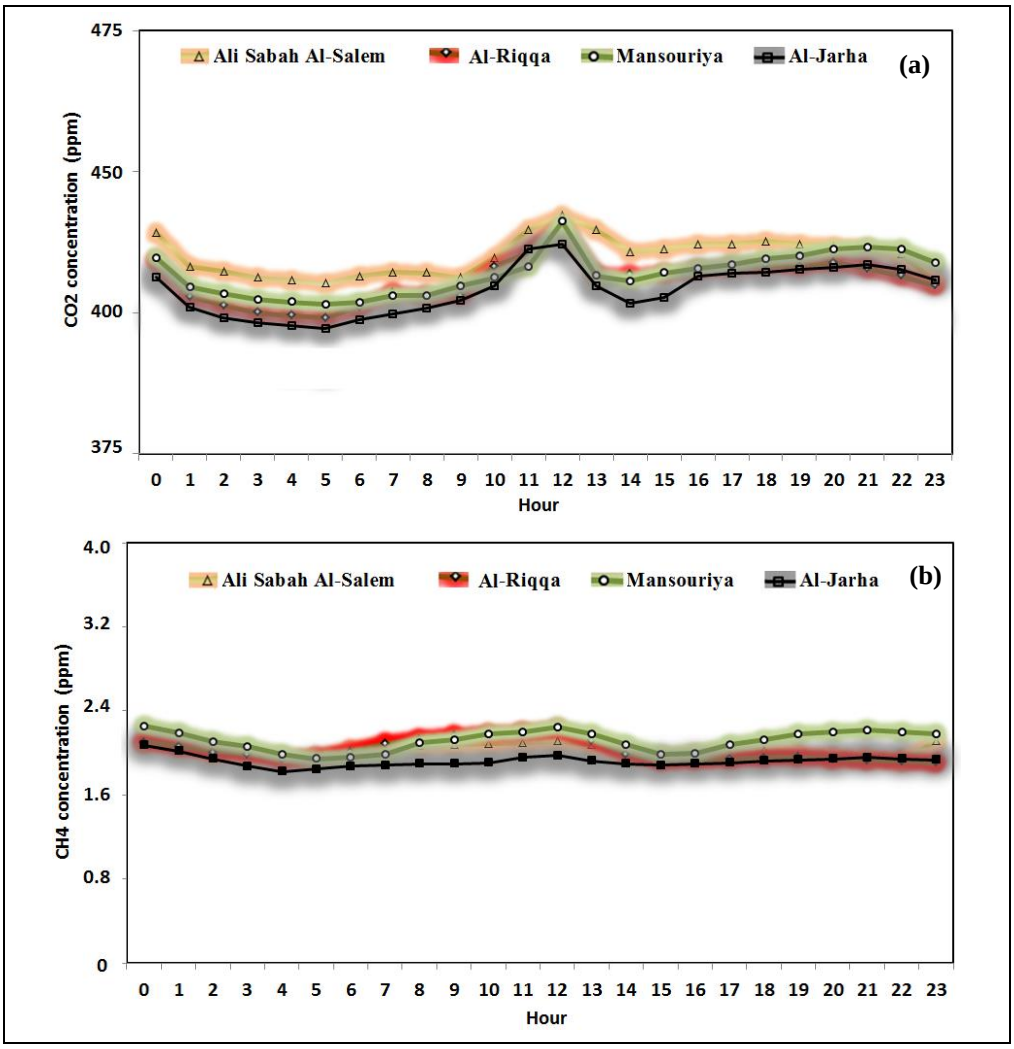

Figure 4. *Diurnal variations of (a) CO_2 and (b) CH_4 concentrations in urban areas in Kuwait*

http://www.aloki.hu ● ISSN 1589 1623 (Print) ● ISSN1785 0037 (Online)
DOI: http://dx.doi.org/10.15666/aeer/1802_20872107

As shown in *Figure 4a*, the increased CO_2 records were observed during three intermittent intervals of day along the entire year; one at near midnight (around 12 am); another at noon time (around 12 pm), and the last between 4 pm and 9 pm. In the latter two periods, high CO_2 levels could be ascribed to busy traffic hours in this study, which is consistent with other urban areas with strong anthropogenic activities, such as vehicular emissions as a result of burning fossil fuels (Aikawa et al., 1995; Takahashi et al., 2002; Gratani and Varone, 2005). While increased level of CO_2 at near midnight (around 12 am) could be possibly attributed to the combined effects of respiration by the living organism and/or from soils, the minimum levels occurred at the night/morning transition between 3 am and 5 am is likely due to decreases anthropogenic CO_2 emissions. Another decrease in CO_2 was observed in the afternoon, which can be attributed to photosynthetic activities (Spittlehouse and Ripley, 1977; Baez et al., 1988; Nasrallah et al., 2003) and the expansion of the mixing height (Aikawa et al., 1995). The CH_4 diurnal cycle was also investigated and the results are shown in *Figure 4b*. The CH_4 diurnal pattern was similar to those observed with CO_2, which implies that both CO_2 and CH_4 have common emission sources. Diurnal results in this study are consistent with other similar studies (Smith et al., 2002; Aikawa et al., 2006; Satar et al., 2016).

Modeling of GHG using artificial neural network (ANN) models

The forecasting of GHG (mainly CO_2 and CH_4) trends has received significant attention in recent years. The International Energy Agency (IEA) reported that 71% of energy-related GHG emissions were attributable to urban areas and it is assumed to grow by 5% by 2030 (IEA, 2008). As mention in methodology section, the number of hidden layers as well as the number of neurons within the hidden layers is usually determined by trial and error. A number of trials were carried out to determine the optimal number of hidden layers, number of neurons in the hidden layers, learning rate, and the learning algorithm. Among several ANN architectures evaluated, five cases are selected and listed in *Table 2*. For the MLP, sigmoidal functions were used whereas Gaussian functions were used for RBF based networks. In searching for the best network weights, conjugate gradient descent was used for MLP. On the other hand, and since two-stage training phase is used for RBF networks, *k*-mean centering and the pseudo-inverse (singular value decomposition) algorithm were used to determine the radial basis functions' parameters and the output layers' weights, respectively. In addition, two positive constants have to be set during the networks learning phase, namely the learning rate and the momentum coefficient. The latter become important especially for networks with large number of inputs-outputs and complex architecture. The rule of the learning rate is to regulate the rate at which the weights are adjusted while the momentum coefficient is a surplus that is added to the adjusted weights to speed up the training. The latter are important to avoid trapping in local minima and an unstable learning (Baughman and Liu, 1995). After several trials, the learning rate and the momentum was set to 0.5 and 0.7, respectively. The observed and predicted values of CO_2 and CH_4 concentrations for the best five models are presented in *Figures 5 and 6*, respectively. Among these five optimal models for each urban area, the best model was selected based on a low value of error mean, absolute error mean, and standard deviation ratio and high correlation coefficients (r). These performance indices differently demonstrate the association between observed and predicted concentration values of CO_2 and CH_4 as predicted by the ANN model as shown in *Table 2*. The higher correlation coefficient showed that the predicted CO_2 and CH_4 concentration values using the ANN model are in good agreement with the observed CO_2

http://www.aloki.hu ● ISSN 1589 1623 (Print) ● ISSN1785 0037 (Online)
DOI: http://dx.doi.org/10.15666/aeer/1802_20872107

and CH_4 concentrations as shown in *Table 2*. The correlation coefficients (r) of the parity plots of the selected optimal models for CO_2 were 0.76, 0.81, 0.72, and 0.73 for areas Ali Sabah Al-Salem, Al-Riqqa, Mansouriya, and Al-Jarha, respectively. For CH_4, the correlation coefficients were 0.77, 0.66, 0.72, and 0.96 for areas Ali Sabah Al-Salem, Al-Riqqa, Mansouriya, and Al-Jarha, respectively. It is worth highlighting that all the optimal models for CO_2 and CH_4 were radial basis function (RBF) network models for all urban cities investigated. The RBF network has shown great promise in this sort of problem due to several of its features, including its very good functional approximation capabilities (Park and Sandberg, 1991), which arise naturally as regularized solutions of ill-posed problems (Poggio and Girosi, 1990) and are utilized well in the theory of interpolation (Powell, 1987). In addition to these features, the intrinsic structure of the RBF network allows learning in stages, which leads to a reduction in training time. This has indeed resulted in the widespread use of RBF networks in numerous practical problems.

Table 2. *Selected ANN models for predictions CO_2 and CH_4 concentrations in the four urban cities*

	CO_2					**CH_4**				
Ali Sabah Al-Salem	**M1**	**M2**	**M3**	**M4**	**M5**	**M1**	**M2**	**M3**	**M4**	**M5**
Error Mean	0.80	0.64	-0.36	-0.61	-0.52	-0.012	-0.017	-0.017	-0.013	-0.003
Error S.D.	18.2	17.9	17.7	15.2	15.3	0.15	0.17	0.18	0.17	0.16
Abs E. Mean	14.8	14.7	14.3	10.92	10.94	0.11	0.13	0.13	0.12	0.12
S.D. Ratio	0.86	0.85	0.84	0.72	0.72	0.71	0.84	0.83	0.80	0.76
Correlation	0.56	0.58	0.60	0.74	0.76	0.77	0.60	0.61	0.68	0.69
Hidden	0	5	6	11	22	34	0	0	3	4
M. Type	L	MLP	MLP	RBF	RBF	RBF	L	L	MLP	MLP
Al-Riqqa	**M1**	**M2**	**M3**	**M4**	**M5**	**M1**	**M2**	**M3**	**M4**	**M5**
Error Mean	0.94	1.06	1.37	1.14	1.26	-0.003	-0.001	-0.003	0.009	-0.006
Error S.D.	22.2	17.3	18.2	17.2	16.4	0.308	0.345	0.345	0.336	0.322
Abs E. Mean	17.15	12.23	14.19	13.06	11.94	0.245	0.279	0.278	0.255	0.250
S.D. Ratio	0.94	0.72	0.76	0.72	0.69	0.841	0.942	0.941	0.915	0.877
Correlation	0.41	0.75	0.70	0.75	0.81	0.66	0.40	0.40	0.50	0.55
Hidden	0	4	5	11	22	34	0	0	5	6
M. Type	L	MLP	MLP	RBF	RBF	RBF	L	L	MLP	MLP
Mansouriya	**M1**	**M2**	**M3**	**M4**	**M5**	**M1**	**M2**	**M3**	**M4**	**M5**
Error Mean	0.87	-1.29	-1.11	0.11	-0.17	-0.01	0.00	0.00	-0.02	-0.01
Error S.D.	27.40	25.32	25.45	23.34	22.55	0.16	0.18	0.18	0.19	0.16
Abs E. Mean	21.26	20.57	20.44	17.75	17.06	0.12	0.14	0.14	0.14	0.12
S.D. Ratio	0.92	0.85	0.85	0.78	0.76	0.75	0.83	0.83	0.86	0.77
Correlation	0.50	0.58	0.58	0.67	0.72	0.72	0.61	0.61	0.56	0.70
Hidden	0	1	3	22	34	34	0	0	1	4
M. Type	L	MLP	MLP	RBF	RBF	RBF	L	L	MLP	MLP
Al-Jarha	**M1**	**M2**	**M3**	**M4**	**M5**	**M1**	**M2**	**M3**	**M4**	**M5**
Error Mean	-0.92	-0.60	0.26	0.19	-0.88	-0.001	0.030	0.031	-0.003	0.024
Error S.D.	7.29	6.91	7.10	7.72	6.71	0.10	0.42	0.42	0.10	0.42
Abs E. Mean	5.61	5.00	5.37	6.01	5.05	0.07	0.21	0.21	0.08	0.17
S.D. Ratio	0.89	0.85	0.87	0.94	0.82	0.24	1.01	1.00	0.25	1.01
Correlation	0.57	0.62	0.55	0.39	0.73	0.96	0.30	0.27	0.96	0.2
Hidden	0	6	34	22	3	34	0	0	1	4
M. Type	L	MLP	RBF	MLP	RBF	RBF	L	L	MLP	MLP

* M1-M5 stands for models' number, L: Linear, MLP: multilayer perception, and RBF: radial basis function

http://www.aloki.hu ● ISSN 1589 1623 (Print) ● ISSN1785 0037 (Online)
DOI: http://dx.doi.org/10.15666/aeer/1802_20872107

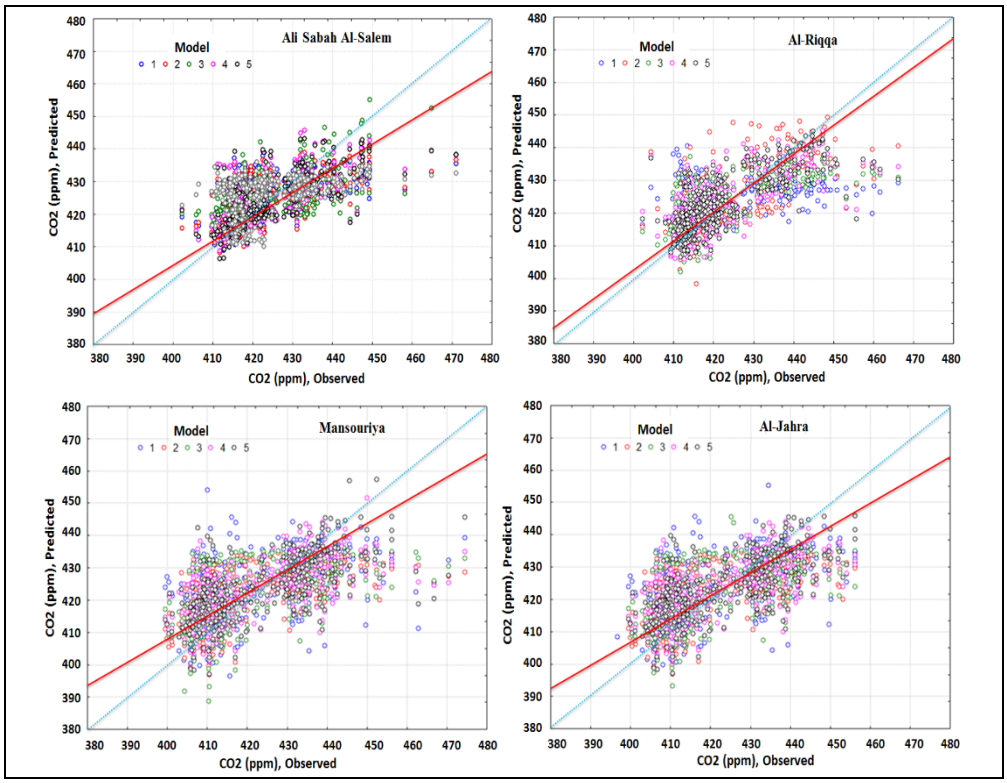

Figure 5. *Comparisons between the observed and predicted daily CO_2 emissions at all sites in 2016. The dashed line is the 1:1 line, and the solid line is the best-fit line*

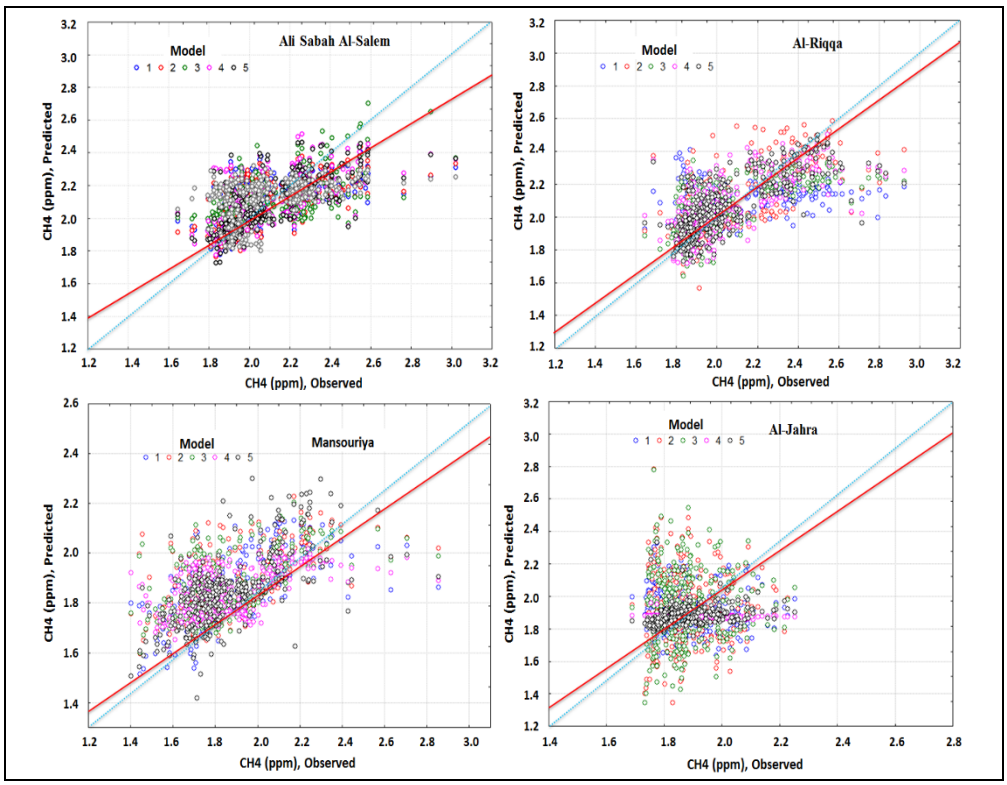

Figure 6. *Comparisons between the observed and predicted daily CH_4 emissions at all sites in 2016. The dashed line is the 1:1 line, and the solid line is the best-fit line*

http://www.aloki.hu ● ISSN 1589 1623 (Print) ● ISSN1785 0037 (Online)
DOI: http://dx.doi.org/10.15666/aeer/1802_20872107

To further check the accuracy of the developed model, a time series plot of the predicted versus the observed for CO_2 and CH_4 is shown in *Figures 7 and 8*. The performance statistics, MAE, RMSE, and FB, of the selected optimal ANN for the four urban areas for CO_2 and CH_4 are given in *Table 3*. The MAE ranged between 5.4 and 15.8 ppm and RMSE varied from 6.9 to 15.5 ppm for CO_2 in all tested urban areas. It is imperative to note that the slightly higher numbers of RMSE in the modeling of CO_2 are due to squaring the errors that tends to heavily weight statistical outliers and therefore a large RMSE may result even though errors may be small and fairly satisfactory elsewhere. Another important point to note is that the annual mean concentration of CO_2 varied between 394 and 425 ppm in the four tested urban areas and, therefore, performance statistics values, differences between the observed and the predicted, listed above represent 1.5% to 4.4% of the total concentrations, which can be deemed acceptable. Concerning CH_4, the MAE values were between 0.11 and 0.21 ppm and RMSE ranged from 0.1 to 0.31 ppm for all tested urban areas. FB was also calculated to test whether predicted values were underestimated (FB>0) or overestimated (FB<0). The FB values for CO_2 and CH_4 approach zero (-0.001 to -0.008 for CO_2 versus -0.001 to -0.04 for CH_4). Overall, the statistical performance indicators reveal that ANN models can estimate CO_2 and CH_4 concentrations in urban areas for the given data set with decent accuracy. To the best knowledge of the authors, there is no nonlinear predictive models that were used in Kuwait to monitor the concentrations levels of CH_4 and CO_2 in the atmosphere. These forecasting models would be beneficial for concerned authorities for planning and proposing environmental legislations to monitor and limit the levels of GHG in Kuwait.

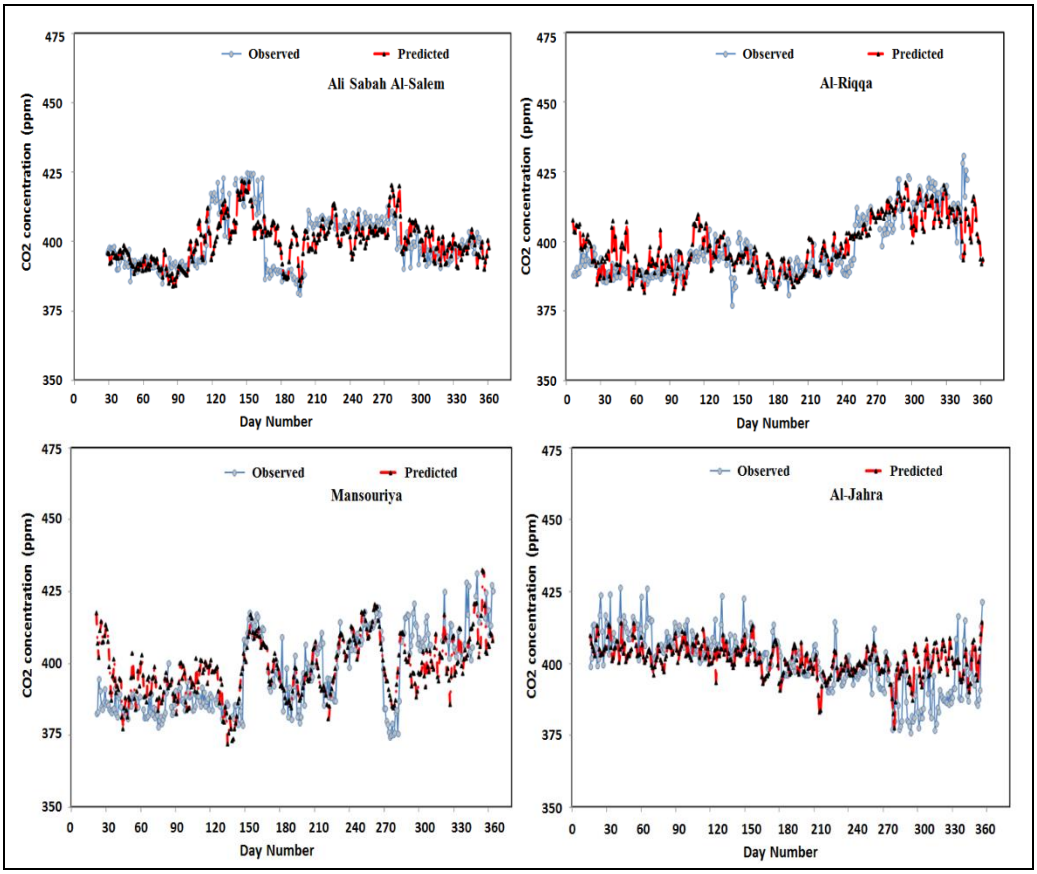

Figure 7. *Daily time series of observed and predicted concentration of CO_2 in four urban cities*

http://www.aloki.hu ● ISSN 1589 1623 (Print) ● ISSN1785 0037 (Online)
DOI: http://dx.doi.org/10.15666/aeer/1802_20872107

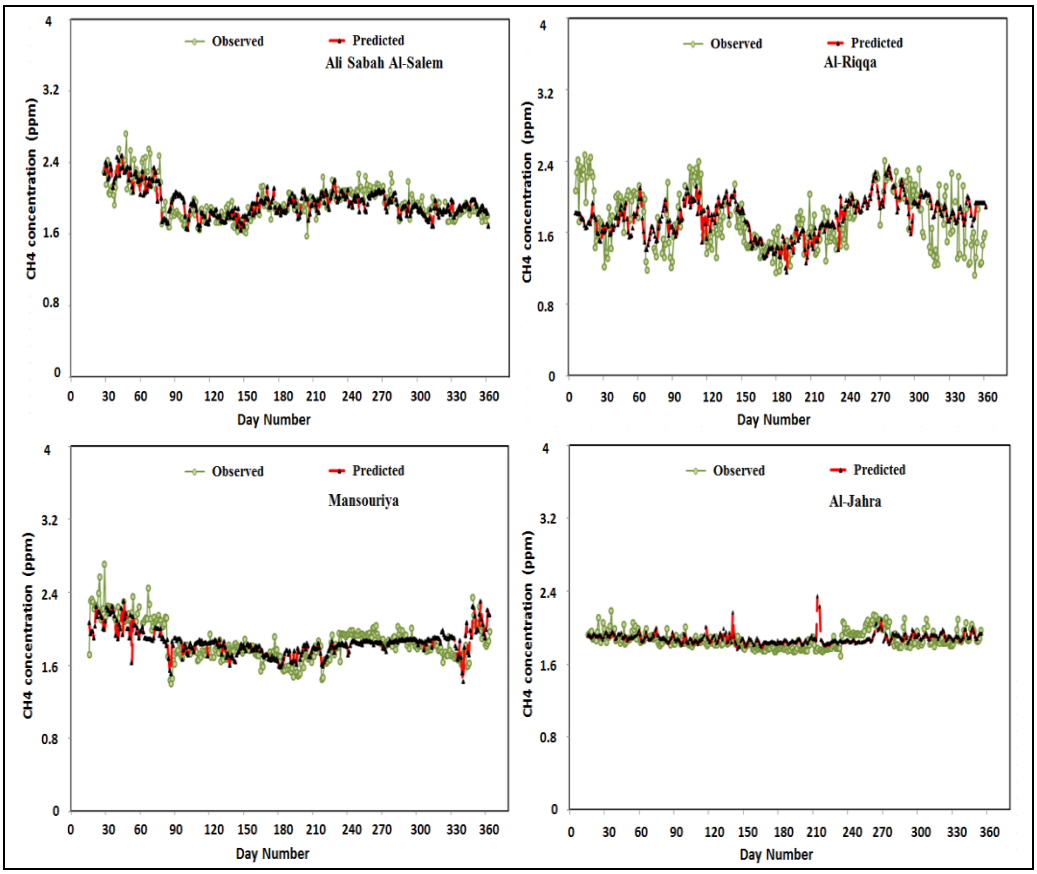

Figure 8. *Daily time series of observed and predicted concentration of CH_4 in four urban cities*

Table 3. *Performance statistical indicators in ppm*

Gases	Statistical indicators	Ali Sabah Al-Salem	Al-Riqqa	Mansouriya	Al-Jarha
CO_2	MAE	11.9	11.2	15.8	5.4
	RMSE	15.5	14.3	19.6	6.9
	FB	-0.002	-0.007	-0.008	-0.001
CH_4	MAE	0.17	0.21	0.11	0.12
	RMSE	0.26	0.31	0.1	0.1
	FB	-0.01	-0.04	-0.001	-0.003

Conclusions

In the present work, GHG emission for 13-year period was investigated in hourly, daily, seasonal, and yearly basis to gain overall picture about the trend of GHG emissions in Kuwait. Records confirmed year-year rising pattern in GHG emissions, higher levels in summer than in winter, due to enormous burning of fossil fuel for cooling purposes and traffic activities. Elevated levels of GHG emissions were observed both at noon and between 4 pm and 9 pm probably ascribed to busy traffic hours while during midnight are likely due to the combined effects of respiration by the living organism and/or from soils. Subsequently and most importantly, the capabilities of multiple linear regression and two types of neural networks, MLP and RBFN for forecasting GHG emissions have been investigated. Among the developed models and based on different statistical

http://www.aloki.hu ● ISSN 1589 1623 (Print) ● ISSN1785 0037 (Online)
DOI: http://dx.doi.org/10.15666/aeer/1802_20872107

performance indices, RBF models outperformed the multiple linear regression and MLP in all urban cities investigated. The RBF exhibited high performance in predicting GHG due to several reasons including its precise functional approximation capabilities and its intrinsic structure that permits learning in stages, which leads to a decrease in training time. This indeed explains the popularity use of RBF networks in numerous practical problems. This study and similar studies would be used as a control tool by government and decision makers for formulation of climate change policies in urban cities compatible with international standpoints.

Acknowledgement. The authors would like to thank Kuwait University and Kuwait Environment Public Authority (KUEPA) for their assitance in data measurments and for continuous support.

REFERENCES

[1] Aikawa, M., Yoshikawa, M., Tomida, M., Aotsuka, F., Haraguchi, H. (1995): Continuous monitoring of the carbon dioxide concentration in the urban atmosphere of Nagoya, 1991-1993. – Analytical Sciences 11: 357-362.

[2] Aikawa, M., Hiraki, T., Eiho, J. (2006): Vertical atmospheric structure estimated by heat island intensity and temporal variations of methane concentrations in ambient air in an urban area in Japan. – Atmospheric Environment 40(23): 4308-4315.

[3] Amoura, K., Wira, P., Djennoune, S. (2011): A state-space neural network for modeling dynamical nonlinear systems. – NCTA 2011 - Proceedings of the International Conference on Neural Computation Theory and Applications: 369-376.

[4] Baez, A., Reyes, M., Rosas, I., Mosiño, P. (1988): CO2 concentrations in the highly polluted atmosphere of Mexico City. – Atmosfera 1: 87-98.

[5] Balch, J., Nagy, R., Archibald, S., Bowman, D., Moritz, M., Roos, C., Scott, A., Williamson, G. (2016): Global combustion: the connection between fossil fuel and biomass burning emissions (1997-2010). – Philos Trans R Soc Lond B Biol Sci 371: 1696-1706.

[6] Baughman, D., Liu, Y. (1995): Neural networks in bioprocessing and chemical engineering. – Academic Press, Inc. USA.

[7] Bergeron, O., Strachan, I. (2011): CO_2 sources and sinks in urban and suburban areas of a northern mid-latitude city. – Atmospheric Environment 45: 1564-1573.

[8] Chandra, N., Lal, S., Venkataramani, S., Patra, P., Sheel, V. (2016): Temporal variations of atmospheric CO_2 and CO at Ahmedabad in western India. – Atmos. Chem. Phys. 16: 6153-6173.

[9] Elangasinghe, M., Singhal, N., Dirks, K., Salmond, J. (2014): Development of an ANN–based air pollution forecasting system with explicit knowledge through sensitivity analysis. – Atmos. Pollut. Res. 5: 696-708.

[10] Elminir, H., Abdel-Galil, H. (2006): Estimation of air pollutants concentrations from meteorological parameters using artificial neural network. – Journal of electrical engineering 57(2): 105-110.

[11] Ghauri, B., Lodhi, A., Mansha, M. (2007): Development of baseline (air quality) data in Pakistan. – Environmental Monitoring Assessment 127: 237-252.

[12] Gratani, L., Varone, L. (2005): Daily and seasonal variation of CO2 in the city of Rome in relationship with the traffic volume. – Atmospheric Environment 39: 2619-2624.

[13] Guclu, D., Dursun, S. (2010): Artificial neural network modelling of a large-scale wastewater treatment plant operation. – Bioprocess Biosyst Eng 33: 1051-1058.

[14] Hassan, M., Dong, Z. (2018): Analysis of Tropospheric Ozone by Artificial Neural Network Approach in Beijing. – Journal of Geoscience and Environment Protection 6: 8-17.

http://www.aloki.hu ● ISSN 1589 1623 (Print) ● ISSN1785 0037 (Online)
DOI: http://dx.doi.org/10.15666/aeer/1802_20872107

[15] International Energy Agency (IEA) (2008): World Energy Outlook 2008. – IEA, Paris, 569 pages.
[16] Intergovernmental Panel on Climate Change (IPCC) (2013): The Physical Science Basis. – In: Stocker, T. F., Qin, D., Plattner, G. K., Tignor, M., Allen, S. K., Boschung, J., Nauels, A., Xia, Y., Bex, V., Midgley, P. M. (eds.) Contribution of Working Group I to the Fifth Assessment Report of the Intergovernmental Panel on Climate Change. Cambridge University Press, Cambridge, United Kingdom and New York, NY, USA, 2013.
[17] Ito, A., Saigusa, N., Murayama, S., Yamamoto, S. (2005): Modeling of gross and net carbon dioxide exchange over a cool-temperate deciduous broad-leaved forest in Japan: Analysis of seasonal and interannual change. – Agricultural and Forest Meteorology 134(1-4): 122-134.
[18] Jędrysek, M., Halas, S., Pieńkos, T. (2015): Carbon Isotopic Composition of Early diagenetic Methane: Variations With Sediments Depth. – Annales UMCS, Physica 69: 29-52.
[19] Karray, F., De Silva, C. (2004): Soft Computing and Intelligent Systems Design. – Addison-Wesley Longman, Inc. UK.
[20] Kumar, A., Dixit, S., Varadarajan, C., Vijayan, A., Masuraha, A. (2006): Evaluation of the AERMOD dispersion model as a function of atmospheric stability for an urban area. – Environmental Progress 25: 141-151.
[21] Kunt, F., Ayturan, Z., Dursun, S. (2016): Used Some Modelling Applications in Air Pollution Estimates. – J. Int. Environmental Application & Science 11: 418-425.
[22] Kurt, A., Oktay, A. (2010): Forecasting air pollutant indicator levels with geographic models 3 days in advance using neural networks. – Expert Systems with Applications 37: 7986-7992.
[23] Loh, Z., Chen, D., Bai, M., Naylor, T., Griffith, D., Hill, J., Denmead, T., McGinn, S., Edis, R. (2008): Measurement of greenhouse gas emissions from Australian feedlot beef production using open-path spectroscopy and atmospheric dispersion modelling. – Aust J Exp Agric 48: 244-247.
[24] Mahmood, I., Iqbal, M., Shahzad, M., Waqas, A., Atique, L. (2016): Spatiotemporal Monitoring of CO_2 and CH_4 over Pakistan Using Atmospheric Infrared Sounder (AIRS). – Int Lett Nat Sci. 58: 35-41.
[25] Mason, S., Baddour, O. (2008): Statistical Modelling. – Troccoli, A., Harrison, M., Anderson, D. L. T., Mason, S. J. (eds.) Seasonal Climate: Forecasting and Managing Risk. NATO Science Series 82, Springer, Dordrecht.
[26] Nasrallah, H., Balling, R., Madi, S., Al Ansari, C. (2003): Temporal variations in atmospheric CO_2 concentration in Kuwait City, Kuwait with comparison to Phoenix, Arizona, USA. – Environmental Pollution 121: 301-305.
[27] Nezhad, A., Mousavi, S., Aghahoseini, S. (2011): Development of an artificial neural network model to predict CO_2 minimum miscibility pressure. – NAFTA 62: 105-108.
[28] Noor, C., Mamat, R., Ahmed, A. (2018): Comparative Study of Artificial NeutralNetwork and Mathematical modelon Marine Diesel Engine Performance Prediction. – International Journal of Innovative Computing, Information and Control 14: 959-969.
[29] Ozcan, H., Ucan, O., Sahin, U., Borat, M., Bayat. C. (2006): Artificial neural network modeling of methane emissions at Istanbul Kemerburgaz-Odayeri Landfill Site. – Journal of Scienfitic and Industrial Research 65: 128-134.
[30] Park, J., Sandberg, I. (1991): Universal approximation using radial basis function networks. – Neural Computation 3(2): 246-257.
[31] Parvizi, B., Khanlarkhani, A., Palizdar, A. (2018): Nonlinear predictive control based on artificial neural network model for pilot reformer plant: Approach for ratio control. – Bulgarian Chemical Communications 50: 286-293.
[32] Patel, V., Kumar, A. (1998): Evaluation of three air dispersion models: ISCST2, ISCLT2 and SCREEN2 for mercury emissions in an urban area. – Environmental Monitoring and Assessment 53: 259-277.

http://www.aloki.hu ● ISSN 1589 1623 (Print) ● ISSN1785 0037 (Online)
DOI: http://dx.doi.org/10.15666/aeer/1802_20872107

[33] Pawul, M., Śliwka, M. (2016): Application of Artificial Neutral Networks for Prediction of Air Pollution levels in Environmental Monitoring. – Journal of Ecological Engineering 17: 190-196.
[34] Poggio, T., Girosi, F. (1990): Networks for approximation and learning. – Proc. IEEE 78(9): 1481-1497.
[35] Powell, M. (1987): Radial basis function for multivariate interpolation. – In: Mason, J. C., Cox, M. G. (eds.) A review algorithms for the approximation of functions and data. Clarendon, Oxford, UK.
[36] Rahimi, A. (2017): Short-term prediction of NO2 and NOx concentrations using multilayer perceptron neural network: a case study of Tabriz, Iran. – Ecol Process 6(4): 1-9.
[37] Riswadkar, R., Kumar, A. (1994): Evaluation of the industrial source complex short-term model in a large-scale multiple source region for different stability classes. – Environmental Monitoring and Assessment 33: 19-32.
[38] Russo, A., Lind, P., Raischel, F., Trigo, R., Mendes, M. (2015): Neural network forecast of daily pollution concentration using optimal meteorological data at synoptic and local scales. – Atmos. Pollut. Res. 6: 540-549.
[39] Sahin, U., Ucan, O., Soyhan, B., Bayat, C. (2004): Modeling of CO distribution in Istanbul using artificial neural network. – Fresen. Environ Bull. 13: 839-845.
[40] Satar, E., Berhanu, T., Brunner, D., Henne, S., Leuenberger, M. (2016): Continuous CO2/CH4/CO measurements (2012–2014) at Beromünster tall tower station in Switzerland. – Biogeosciences 13: 2623-2635.
[41] Shim, C., Han, J., Henze, D., Yoon, T. (2018): Identifying local anthropogenic CO2 emissions with satellite retrievals: a case study in South Korea. – International Journal of Remote Sensing. DOI: 10.1080/01431161.2018.1523585.
[42] Sikar, E., La Scala, N. (2004): Methane and Carbon Dioxide Seasonal Cycles at Urban Brazilian Inland Sites. – Journal of Atmospheric Chemistry 47(2): 101-106.
[43] Smith, F., Elliott, S., Blake, D., Rowland, F. (2002): Spatiotemporal variation of methane and other trace hydrocarbon concentrations in the Valley of Mexico. – Environmental Science & Policy 5: 449-461.
[44] Spittlehouse, D., Ripley, E. (1977): Carbon dioxide concentrations over a native grassland in Saskatchewan. – Tellus 29: 54-65.
[45] Sterman, J. D., Siegel, L., Rooney-Varga, J. N. (2018): Does replacing coal with wood lower CO2 emissions? Dynamic life cycle analysis of wood bioenergy. – Environ. Res. Lett. 13:015007.
[46] Tahboub, K. K., Barghash, M., Arafeh, M., Ghazal, O. (2016): An ANN-GA Framework for Optimal Engine Modeling. – Mathematical Problems in Engineering 2016:6180758.
[47] Takahashi, H., Konohira, E., Hiyama, T., Minami, M., Nakamura, T., Yoshida, N. (2002): Diurnal variation of CO2 concentration, δ14C and δ13C in an urban forest: estimate of the anthropogenic and biogenic contributions. – Tellus 54B: 97-109.
[48] The World Data Centre for Greenhouse Gases (WDCGG) (2018): https://gaw.kishou.go.jp /search. (Accessed in 16/12/2018).
[49] Walsh, B., Ciais, P., Janssens, I., Pen˜uelas, J., Riahi, K., Rydzak, F., Vuuren, D. P., Obersteiner, M. (2017): Pathways for balancing CO2 emissions and sinks. – Nat. Commun. 8(14856): 1-12.
[50] World Meteorological Organization (WMO) (2017): WMO Greenhouse Gas Bulletin No.13. – https://library.wmo.int/doc_num.php?explnum_id=4022.
[51] Wu, S., Feng, Q., Du, Y., Li, X. (2011): Artificial neural network models for daily PM10 air pollution index prediction in the urban area of Wuhan. – China. Environ. Eng. Sci. 28: 357-363.
[52] Zhang, J., Feng, Q., Wang, S., Zhang, X., Wang, S. (2016): Estimation of CO2–brine interfacial tension using an artificial neural network. – J. of Supercritical Fluids 107: 31-37.

http://www.aloki.hu ● ISSN 1589 1623 (Print) ● ISSN1785 0037 (Online)
DOI: http://dx.doi.org/10.15666/aeer/1802_20872107

[53] Zhang, J., Ding, W. (2017): Prediction of Air Pollutants Concentration Based on an Extreme Learning Machine: The Case of Hong Kong. – Int J Environ Res Public Health 14(114): 1-19.
[54] Zhao, H., Wang, Y., Song, J., Gao, G. (2018): The pollutant concentration prediction model of NNP-BPNN based on the INI algorithm, AW method and neighbor-PCA. – Journal of Ambient Intelligence and Humanized Computing. https://doi.org/10.1007/s12652-018-0837-9.

http://www.aloki.hu ● ISSN 1589 1623 (Print) ● ISSN1785 0037 (Online)
DOI: http://dx.doi.org/10.15666/aeer/1802_20872107